Power and energy scaling of a diode-end-pumped Nd:YLF laser through gain optimization

Christoph Bollig,[1,2*] Cobus Jacobs,[1,3] M. J. Daniel Esser,[1] Edward H. Bernhardi,[1,4] and Hubertus M. von Bergmann[2]

[1] *National Laser Centre, Council for Scientific and Industrial Research (CSIR), Pretoria 0001, South Africa,*
[2] *Laser Research Institute, Physics Department, University of Stellenbosch, Stellenbosch 7602, South Africa*
[3] *Department of Electrical and Electronic Engineering, University of Stellenbosch, Stellenbosch 7602, South Africa*
[4] *School of Physics, University of Kwazulu-Natal, Durban 4000, South Africa*
**cbollig@csir.co.za*

Abstract: An end-pumped Nd:YLF laser was demonstrated, which delivered 60.3 W continuous-wave and more than 52 W *Q*-switched average power for all repetition rates from 5 to 30 kHz. To achieve this, an analytical solution to estimate and optimize the unsaturated gain in an end-pumped laser gain medium was derived. The approach presented here should open up the route for scaling end-pumped lasers to even higher power and energy levels.

OCIS codes: (140.3480) Lasers, diode-pumped; (140.3540) Lasers, Q-switched; (140.3530) Lasers, neodymium

References and links

1. V. Bagnoud, M. J. Guardalben, J. Puth, J. D. Zuegel, T. Mooney, and P. Dumas, "High-energy, high-average-power laser with Nd:YLF rods corrected by magnetorheological finishing," Appl. Opt. **44**(2), 282–288 (2005).
2. H. Vanherzeele, "Continuous wave dual rod Nd:YLF laser with dynamic lensing compensation," Appl. Opt. **28**(19), 4042–4044 (1989).
3. A. Dergachev, and P. F. Moulton, "Short-pulse, high-repetition rate, high-power Nd:YLF MOPA system," in *Advanced Solid-State Photonics* (TOPS), G. Quarles, ed., Vol. **94** of OSA Trends in Optics and Photonics, paper 191 (Optical Society of America, 2004).
4. A. Dergachev, J. H. Flint, Y. Isyanova, B. Pati, E. V. Slobodtchikov, K. F. Wall, and P. F. Moulton, "Review of Multipass Slab Laser Systems," IEEE J. Sel. Top. Quantum Electron. **13**(3), 647–660 (2007).
5. N. U. Wetter, E. C. Sousa, F. A. Camargo, I. M. Ranieri, and S. L. Baldochi, "Efficient and compact diode-side-pumped Nd:YLF laser operating at 1053 nm with high beam quality," J. Opt. A, Pure Appl. Opt. **10**(10), 104013 (2008).
6. H. Zhang, D. Li, P. Shi, R. Diart, A. Shell, C. R. Haas, and K. Du, "Efficient, high power, Q-switched Nd:YLF slab laser end-pumped by diode stack," Opt. Commun. **250**(1-3), 157–162 (2005).
7. D. Li, Z. Ma, R. Haas, A. Schell, P. Zhu, P. Shi, and K. Du, "Diode-end-pumped double Nd:YLF slab laser with high energy, short pulse width, and diffraction-limited quality," Opt. Lett. **33**(15), 1708–1710 (2008).
8. H. Zbinden, and J. E. Balmer, "Q-switched Nd:YLF laser end pumped by a diode-laser bar," Opt. Lett. **15**(18), 1014–1016 (1990).
9. R. Lavi, S. Jackel, S. Tsadka, O. Levi, and R. Lallouz, "Comparison between Nd:YAG and Nd:YLF laser oscillators, end pumped by high brightness diode laser arrays," SPIE **1971**, 326–336 (1992).
10. W. A. Clarkson, P. J. Hardman, and D. C. Hanna, "High-power diode-bar end-pumped Nd:YLF laser at 1.053 microm," Opt. Lett. **23**(17), 1363–1365 (1998).
11. X. Peng, L. Xu, and A. Asundi, "High-power efficient continuous-wave TEM_{00} intracavity frequency-doubled diode-pumped Nd:YLF laser," Appl. Opt. **44**(5), 800–807 (2005).
12. L. McDonagh, R. Wallenstein, R. Knappe, and A. Nebel, "High-efficiency 60 W $TEM_{(00)}$ Nd:$YVO_{(4)}$ oscillator pumped at 888 nm," Opt. Lett. **31**(22), 3297–3299 (2006).
13. L. McDonagh, R. Wallenstein, and R. Knappe, "47 W, 6 ns constant pulse duration, high-repetition-rate cavity-dumped Q-switched $TEM_{(00)}$ Nd:$YVO_{(4)}$ oscillator," Opt. Lett. **31**(22), 3303–3305 (2006).
14. L. McDonagh, and R. Wallenstein, "Optimized pumping of neodymium-doped vanadate yields high-power lasers," SPIE Newsroom, DOI: 10.1117/2.1200707.0708, *http://spie.org/x15068.xml* (2007)
15. X. Yan, Q. Liu, X. Fu, H. Chen, M. Gong, and D. Wang, "High repetition rate dual-rod acousto-optics Q-switched composite Nd:YVO_4 laser," Opt. Express **17**(24), 21956–21968 (2009).
16. Q. Liu, X. Yan, X. Fu, M. Gong, and D. Wang, "183 WTEM_{00} mode acoustic-optic Q-switched MOPA laser at 850 kHz," Opt. Express **17**(7), 5636–5644 (2009).

#125628 - $15.00 USD Received 17 Mar 2010; revised 14 May 2010; accepted 16 May 2010; published 15 Jun 2010

17. J. R. Ryan, and R. Beach, "Optical absorption and stimulated emission of neodymium in yttrium lithium fluoride," J. Opt. Soc. Am. B **9**(10), 1883–1887 (1992).
18. P. J. Hardman, W. A. Clarkson, G. J. Friel, M. Pollnau, and D. C. Hanna, "Energy-transfer upconversion and thermal lensing in high-power end-pumped Nd:YLF laser crystals," IEEE J. Quantum Electron. **35**(4), 647–655 (1999).
19. M. J. D. Esser, C. Bollig, and H. M. von Bergman, "Efficient power scaling of an end-pumped Nd:YLF laser at 1053 nm," in *EPS-QEOD Europhoton Conference Lausanne,* Europhysics Conference Abstracts Volume **28C**, paper Sol-10139 (2004).
20. W. Koechner, *Solid-state laser engineering* 5th ed. (Springer, 1999), Chap. 8.
21. N. Coluccelli, G. Galzerano, P. Laporta, D. Parisi, A. Toncelli, and M. Tonelli, "Room-temperature Q-switched Tm:$BaY_{(2)}F_{(8)}$ laser pumped by CW diode laser," Opt. Express **14**(4), 1518–1523 (2006).
22. M. Pollnau, P. J. Hardman, W. A. Clarkson, and D. C. Hanna, "Upconversion, lifetime quenching, and ground-state bleaching in Nd^{3+}:$LiYF_4$," Opt. Commun. **147**(1-3), 203–211 (1998).
23. J. D. Zuegel, and W. Seka, "Upconversion and reduced $^4F_{3/2}$ upper-state lifetime in intensely pumped Nd:YLF," Appl. Opt. **38**(12), 2714–2723 (1999).
24. L. Fornasiero, T. Kellner, S. Kück, J. P. Meyn, P. E. A. Möbert, and G. Huber, "Excited state absorption and stimulated emission of Nd^{3+} in crystals III: $LaSc_3(BO_3)_4$, $CaWO_4$, and$YLiF_4$," Appl. Phys. B **68**(1), 67–72 (1999).
25. J. L. Blows, T. Omatsu, J. Dawes, H. Pask, and M. Tateda, "Heat generation in Nd:YVO_4 with and without laser action," IEEE Photon. Technol. Lett. **10**(12), 1727–1729 (1998).
26. T. Y. Fan, and R. L. Byer, "Diode laser-pumped solid-state lasers," IEEE J. Quantum Electron. **24**(6), 895–912 (1988).
27. A. E. Siegman, *Lasers* (University Science Books, 1986); Eqs. (40) and 54, pp. 280, 287.
28. C. Czeranowsky, "Resonatorinterne Frequenzverdopplung von diodengepumpten Neodym-Lasern mit hohen Ausgangsleistungen im blauen Spektralbereich," PhD thesis, University of Hamburg (2002).
29. O. Svelto, *Principles of Lasers* 4th ed. (Springer, 1998); Section 2.9.2 and Appendix C.
30. W. A. Clarkson, "Thermal effects and their mitigation in end-pumped solid-state lasers," J. Phys. D Appl. Phys. **34**(16), 2381–2395 (2001).
31. R. Paschotta, "Beam quality deterioration of lasers caused by intracavity beam distortions," Opt. Express **14**(13), 6069–6074 (2006).
32. S. C. I. O. P. T. Enterprises, "PARAXIA-Plus" (v1.04) [computer program], San Jose, USA, available from: http://www.sciopt.com/paraxpls.htm [Accessed Jan 2010].
33. E. H. Bernhardi, "Modelling diode-pumped solid-state lasers," MSc thesis, University of Kwazulu-Natal (2008).
34. E. H. Bernhardi, C. Bollig, M. J. D. Esser, A. Forbes, L. R. Botha, and C. Jacobs, "A single-element plane-wave solid-state laser rate equation model," S. Afr. J. Sci. **104**, 389–393 (2008).
35. C. Bollig, W. Koen, H. Strauss, and E. Bernhardi, L, R. Botha, D. Esser, and D. Preussler, "Exploiting the natural doping gradient of Nd:YLF crystals for high-power end-pumped lasers," in *EPS-QEOD Europhoton Conference Paris 2008,* Europhysics Conference Abstracts, paper TUp.20 (2008).

1. Introduction

Nd:YLF has been a work horse in the field of solid-state lasers over the past decades. Nd:YLF lasers have been operated in many architectures, e.g. side-pumped by flash lamps [1] or arc-lamps [2], diode-side-pumped slab lasers with multi-pass geometry [3,4] or total internal reflection bounce geometry [5], end-pumped slab lasers with hybrid-unstable geometry [6,7], or end-pumped rod lasers [8–11].

Diode-end-pumped lasers have the advantage of offering high efficiency and good beam quality at the same time. The recent development in high-power high-brightness fiber-coupled diode lasers operating around 800 nm opened up the potential for power scaling diode-end-pumped configurations. This potential has so far mainly been utilized in end-pumped Nd-vanadate (Nd:YVO_4 or Nd:$GdVO_4$) lasers operating CW or *Q*-switched at high repetition rates of tens to hundreds of kHz [12–16]. For *Q*-switched operation at lower repetition rates, Nd:YLF is a more attractive material due to its longer upper laser level lifetime τ of ~525 µs [17]. An additional advantage of Nd:YLF is its very weak thermal lens on the σ-polarization [18].

Previously, diode-end-pumped Nd:YLF lasers with TEM_{00} CW powers of 28.6 and 26.4 W were demonstrated by Peng et al. [11] and by our own group [19], respectively, when pumped with two 30 W fiber-coupled laser diode modules. To our knowledge, the maximum *Q*-switched pulse energy reported so far for a continuously diode-end-pumped Nd:YLF laser was 3 mJ [19]. Since Nd:YLF has a tendency to fracture under high pump powers [10] it is often regarded as not suitable for scaling to very high power levels. Here, we report a concept to scale a diode-end-pumped Nd:YLF laser to higher average powers and higher energies per pulse.

#125628 - $15.00 USD Received 17 Mar 2010; revised 14 May 2010; accepted 16 May 2010; published 15 Jun 2010

2. Background

The theoretical pulse energy of a continuously pumped four-level laser *Q*-switched at low repetition rates (repetition rates well below the inverse lifetime) is more than τP_{cw}, where P_{cw} is the CW power of the same laser (see Eq. (7) below and [20,21]). Unlike in side-pumped and slab lasers, actual pulse energies achieved at low repetition rates in high-power end-pumped lasers usually remain well below this value [e.g 10,13,15,16,19.]. This phenomenon is often attributed to "lifetime quenching," and sometimes an "effective lifetime" is assumed.

We propose that in high-power continuously end-pumped lasers the typical small gain volume compared to side-pumped and slab lasers causes the reduced pulse energy at low repetition rates, mainly due to two phenomena:

- Inter-ionic upconversion, leading to a reduction in stored energy and additional heat generation [22,23].
- A very high unsaturated gain in the laser material leading to *Q*-switch leakage and pulse-build-up times faster than the *Q*-switch opening time when an acousto-optic *Q*-switch is used [10].

Amplified spontaneous emission (ASE) should in general not be a significant problem in high-power end-pumped lasers, as will be discussed in more detail further below. Excited-State Absorption (ESA) is negligible in Nd:YLF at 1053 nm on the σ-polarization [24] and can therefore be excluded as problem for the experiments discussed here.

Inter-ionic upconversion (also referred to as energy-transfer upconversion, ETU) has been identified as a limiting factor in high-power end-pumped solid-state lasers including Nd:YAG, Nd:YLF [10,22,23] and Nd-vanadate [25] lasers. To overcome the effect of upconversion, the doping concentration of the laser material can be reduced and the pumped volume increased. Similar to [11], we used Nd:YLF rods of 0.5% concentration (atomic), which leads to a significant reduction in upconversion compared to the typically used 0.7 to 1% [10,19]. While the lower doping concentration already increases the pumped volume, it can be further increased by pumping on the weaker absorption at 805 nm (e.g [4].) and by increasing the pump beam diameter together with the TEM_{00} mode size in the crystal.

3. Gain analysis

An increased pump and TEM_{00} laser mode size also addresses the second effect, namely too high gain. In order to estimate the optimum pump and TEM_{00} laser beam radii, we have analyzed the gain with an analytical formalism. To calculate the gain, we modified the formalism developed by Fan and Byer to calculate the threshold of a diode-end-pumped laser [26]. They assume that losses are low and follow a low-gain approximation. This cannot be assumed under the conditions analyzed here. All other assumptions are the same, including a Gaussian distribution of the pump and laser mode, no diffraction spreading of the pump and upconversion, ESA and ASE are ignored. This is only a valid assumption for large pumped volumes and low doping concentrations, as discussed above.

In order to take high gain into account, it is necessary to use the exponential form for the round-trip gain G_r (double-pass and not taking into account any losses) as in [27]:

$$G_r = \exp\left(2\sigma \Delta N L\right), \tag{1}$$

where σ is the cross section of the transition, L the length of the active medium and ΔN is the difference of the population of the upper and the lower laser level. It is worth to note that G is a multiplicative factor, e.g. a gain of + 100% would mean that $G = 2$. For an end-pumped laser, the spatial distribution of the inversion and the laser cavity mode have to be taken into account. This can be done by replacing ΔN with $\Delta N(r,z)$ and calculating an overlap integral, which averages the inversion of the laser cavity mode. The round-trip gain is then

$$G_r = \exp\left(2\sigma L \iiint s_0(r,z)\Delta N(r,z)dV\right). \tag{2}$$

#125628 - $15.00 USD Received 17 Mar 2010; revised 14 May 2010; accepted 16 May 2010; published 15 Jun 2010

where $s_0(r,z)$ is the normalized laser cavity mode intensity distribution in the gain medium.

In order to calculate the unsaturated gain at low repetition rates at the time just before a pulse is triggered, we assume that the laser inversion reaches a steady state but that the losses are high enough to prevent laser oscillation (i.e. there is no extraction of energy through stimulated emission). In this case, the same rate equation for the upper laser level population N_b can be used as Eqs. (2) and (3) in [26]. Substituting these into Eq. (2) above, the unsaturated round-trip gain for a four-level laser is

$$G_r = \exp\left(\frac{2\sigma_e L\eta_p P_a \tau}{h\nu_p}\iiint s_0(r,z)r(r,z)dV\right), \tag{3}$$

where τ is the upper manifold lifetime and $r_p(r,z)$ is the normalized pump intensity distribution in the gain medium. P_a is the absorbed pump power, $h\nu_p$ is the pump photon energy and η_p is the pump quantum efficiency, i.e. the number of ions in the upper manifold created per absorbed pump photon. σf_b of [26] has been substituted by the effective stimulated emission cross section σ_e.

In [26] it was shown, that for Gaussian pump and laser beam modes with negligible diffraction, the integral can be solved as

$$\iiint s_0(r,z)r(r,z)dV = \frac{2}{\pi(w_0^2 + w_p^2)L}, \tag{4}$$

where w_0 and w_p are the Gaussian beam radii of the pump and laser beam, respectively. They also point out that this "is not highly dependent on the exact form of $r_p(r,z)$ as long as the power can be described as being within some radius $r = w_p$."

Substituting Eq. (4) into Eq. (3), the unsaturated round-trip gain is

$$G_r = \exp\left(\frac{4P_a}{\pi(w_0^2 + w_p^2)K}\right), \tag{5a}$$

with

$$K = \frac{h\nu_p}{\sigma_e \eta_p \tau}, \tag{5b}$$

where the constant K contains all the material parameters including the pump quantum efficiency η_p. If we assume $\eta_p = 0.7$ for Nd:YLF [26] and use $\sigma_e = 22\times10^{-20}$ cm^2 for the π-polarization and $\sigma_e = 14\times10^{-20}$ cm^2 for the σ-polarization [28], we get K = 31 W/mm^2 and K = 49 W/mm^2 for the two polarizations, respectively.

For an end-pumped laser, a good overlap between the pump beam and the TEM_{00} laser mode is required for high efficiency and good beam quality. Therefore, we will use $w = w_p = w_l$ from now on. This makes the gain even simpler:

$$G_r = \exp\left(\frac{2P_a}{\pi w^2 K}\right) \text{for round-trip gain,} \tag{6a}$$

$$G_s = \exp\left(\frac{P_a}{\pi w^2 K}\right) \text{for single-pass gain.} \tag{6b}$$

#125628 - $15.00 USD Received 17 Mar 2010; revised 14 May 2010; accepted 16 May 2010; published 15 Jun 2010

If πw^2 is viewed as an effective area of the Gaussian beams, then K can be interpreted as the pump power density required to achieve a single-pass unsaturated gain of e or a double-pass unsaturated gain of e^2.

Figure 1 shows the double-pass unsaturated gain G versus laser and pump beam radius w for an assumed absorbed pump power of P_a = 135 W (the maximum in our experiment). It can clearly be seen that the pump and laser beam radii have a very strong influence on the gain. For a radius of w = 0.5 mm, the theoretical gain is ~65,000 for the π-polarization at 1047 nm and ~1,150 for the σ-polarization at 1053 nm. It is obviously unrealistic to achieve this high gain in reality, since other effects like upconversion will reduce the gain at such high pump intensities. For a radius of w = 1 mm, these values are reduced to 16 and 6, respectively.

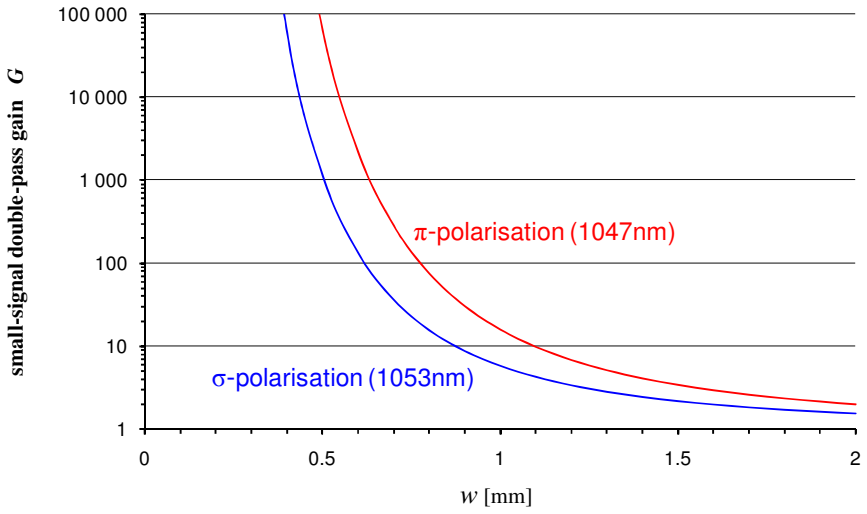

Fig. 1. Theoretical Nd:YLF unsaturated round-trip gain G vs pump and laser beam radius w for 135 W of absorbed pump power, assuming that the pump and laser beams are of equal sizes and that no diffraction takes place in the laser material. Upconversion and ASE are neglected (see text).

In order to operate a laser Q-switched at low repetition rates under continuous pumping, the Q-switch has to provide sufficient loss to completely prevent laser operation under full pump power. This means that the overall round-trip gain has to be below 1, i.e. that $G_s^2 R_{OC} (1 - L)^2 < 1$, where R_{OC} is the output coupler reflectivity and L is the single-pass loss. Figure 2 shows the required Q-switch loss assuming an absorbed pump power of 135 W, an output coupler transmission of 20% and no other losses. Also shown is the theoretical pump power threshold as percentage of the full pump power, according to Eq. (7) in [26]. At w = 0.5 mm, a Q-switch loss of 99.6% and 96.7% is required to suppress operation at the π and σ polarization, respectively. This can only be achieved with Electro-Optic Modulators (EOMs) and not with standard Acousto-Optic Modulators (AOMs), which are cheaper and more suitable for higher repetition rates. However, at w = 1 mm, a Q-switch loss of only 72% and 54% is required to suppress operation at the π and σ polarization, respectively. This falls into the range which can well be achieved with commercial fused-silica AOMs. At the same time, the pump power threshold is only 8% and 13% of the available pump power for the two polarizations, respectively. This is low enough to ensure efficient operation of the laser.

#125628 - $15.00 USD Received 17 Mar 2010; revised 14 May 2010; accepted 16 May 2010; published 15 Jun 2010

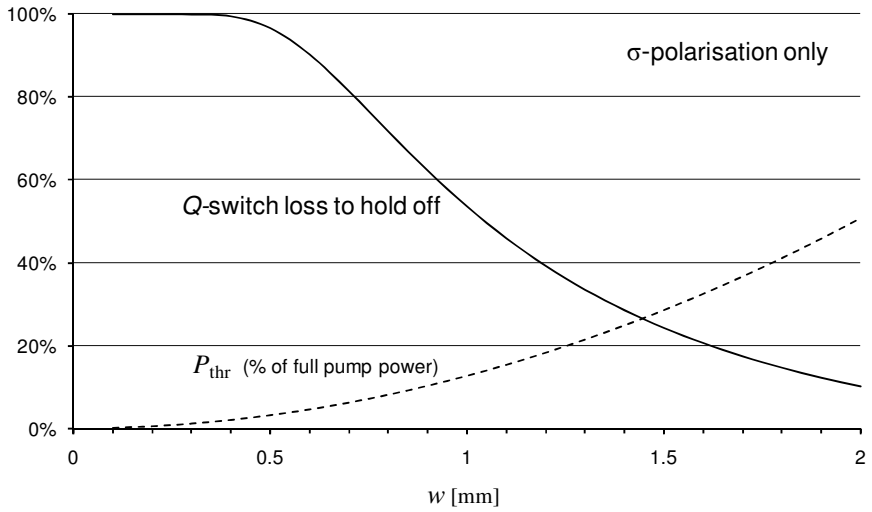

Fig. 2. Solid line: Theoretical minimum single-pass *Q*-switch loss required to prevent lasing on the σ-polarisation under full pump power (135W absorbed). Dotted line: Theoretical threshold pump power as percentage of full pump power versus pump and laser beam radius *w* for an output coupler transmission of 20%.

In order to analyze whether ASE would be a problem for our design described below, the approach suggested by Svelto was followed [29]. To simplify the analysis, we assume that the pump power of 75 W incident on each of the two crystals is absorbed uniformly over the estimated effective pump absorption length in the crystal (~14 mm). In this case, the ASE emission would be ~100 mW at a pump beam radius of w = 1 mm. This demonstrates that ASE will be insignificant in our setup.

4. Experimental setup

4.1 Pump setup

The traditional approach for multi-Watt solid-state lasers end-pumped by a fiber-coupled diode module is to collimate the fiber output with a first lens and then focus it into the crystal with a second lens (e.g [12].). In such a setup, the focus is typically at the geometrical image plane of the fiber end. At the end of the highly multi-mode pump delivery fiber, the intensity distribution is relatively uniform across the core. Therefore, the pump beam has a transverse intensity distribution at the waist in the crystal, which is roughly a top-hat distribution as well.

It has been shown that a top-hat intensity profile of the pump reduces thermal aberrations in materials which exhibit a strong thermal lens, such as Nd:YAG [30]. However, to utilize this advantage, the laser mode has to be ~20% smaller than the pump mode, which results in reduced efficiency. We propose that for a material with a weak thermal lens, and therefore weak aberrations, it would be advantageous to match the Gaussian profile of the laser mode with a roughly bell-shaped pump intensity profile of similar size, since this leads to a better overlap efficiency. In addition, a bell-shaped gain distribution will reduce resonant transverse mode coupling [31] and should provide some degree of soft aperture, which should result in more stable operation when the resonator is close to the stability edge.

In the setup discussed here, we used a pump scheme, which results in a roughly bell-shaped transverse intensity distribution at the pump beam waist in the crystal. This scheme utilizes the fact that the far-field distribution of the fiber is roughly bell-shaped, even for highly multi-mode fibers. The fiber end face is imaged with a lens with relatively short focal length onto the plane of a second lens, as schematically shown in Fig. 3. The transverse intensity distribution on that second lens is then similar to the top-hat function. The second lens focuses the light into the laser gain material, where it will then have an intensity

#125628 - $15.00 USD Received 17 Mar 2010; revised 14 May 2010; accepted 16 May 2010; published 15 Jun 2010

distribution similar to the far-field distribution of the fiber but reduced to a small size. In effect, the second lens images the intensity distribution at the first lens into the fiber.

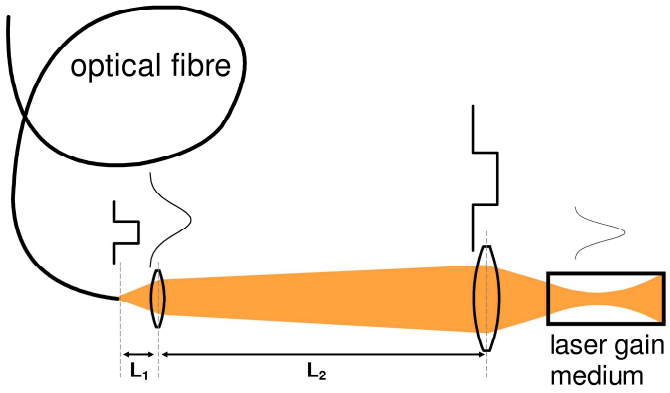

Fig. 3. Simplified diagram of the pump scheme which generates a bell-shaped transverse intensity distribution in the waist of the pump beam. Also shown are the transverse intensity distributions at the different positions along the pump beam. See text for details.

To calculate suitable values for the focal lengths of the two lenses and for the distances, the beam propagation was calculated in Paraxia Plus [32]. For this calculation, the Paraxia "input beam" parameters were set to be a waist at the fiber exit face with a radius of 300 µm and an M^2 of 260. L_1 and L_2 (Fig. 3) were then adjusted to get the correct waist radius at the pump focus, while maintaining the condition that $1/f_1 = 1/L_1 + 1/L_2$. With $f_1 = 25$ mm and $f_2 = 100$ mm, this was achieved for $L_1 = 25.96$ mm and $L_2 = 676$ mm. In this scenario, the pump focus has a radius of 1000 µm and is $L_3 = 116$ mm from the second lens.

The pump diode used was a fiber-coupled diode module with a nominal output power of 140 W (Jenoptik model JOLD-140-CAXF-6A). At full current, it delivered up to 158 W out of the 0.6 mm, 0.22 NA fiber. The pump beam was split into two parts to pump two separate 40 mm long, 0.5% doped Nd:YLF crystals, each from one end. Figure 4 shows the actual pump setup used in this experiment. The pump beam was split in such a way that the distance to the second lens is roughly the same in both pump arms. The beam splitter had a measured reflectivity of 55% at 805 nm. Due to losses on the 1053-nm λ/2 plate, which was only AR-coated for 1053 nm and not for 805 nm, the incident pump power was roughly the same for both crystals. The total pump power incident on the crystals was ~90% of the diode power with ~95% of the incident power absorbed in the crystals, i.e. a total of 135 W was absorbed in both crystals at full pump power.

#125628 - $15.00 USD Received 17 Mar 2010; revised 14 May 2010; accepted 16 May 2010; published 15 Jun 2010

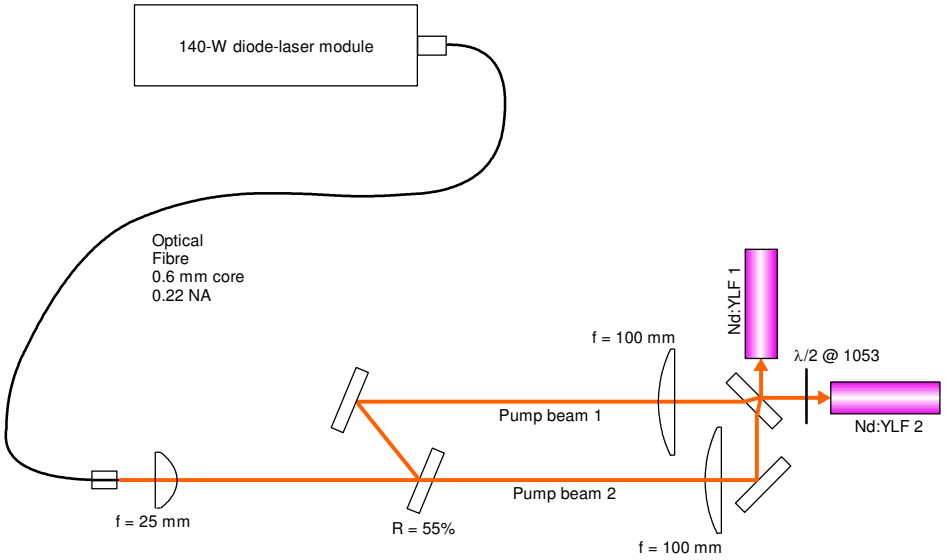

Fig. 4. Pump setup to pump two Nd:YLF crystals.

4.2 Resonator design

Figure 5 shows a diagram of the 773 mm long laser resonator used for both the CW and the *Q*-switched experiments. In order to achieve a large fundamental mode size in the crystals, a folded resonator with a long collimated arm and a short arm was used. It is similar to the resonator described in [10], but with a convex (R = −50 mm) end mirror of the short arm instead of a flat mirror. This reduces the required short-arm length and at the same time significantly increases the beam size on the end mirror of the short arm, thus reducing the risk of damage. The concave folding mirror M_2 had a curvature of 250 mm. Such a resonator has the advantage, that the mode size in the laser crystal can be adjusted by a small variation of the short-arm length L1 around the stability boundary at L = 75 mm. This adjustment can also be used to compensate for the thermal lens generated in the Nd:YLF crystals.

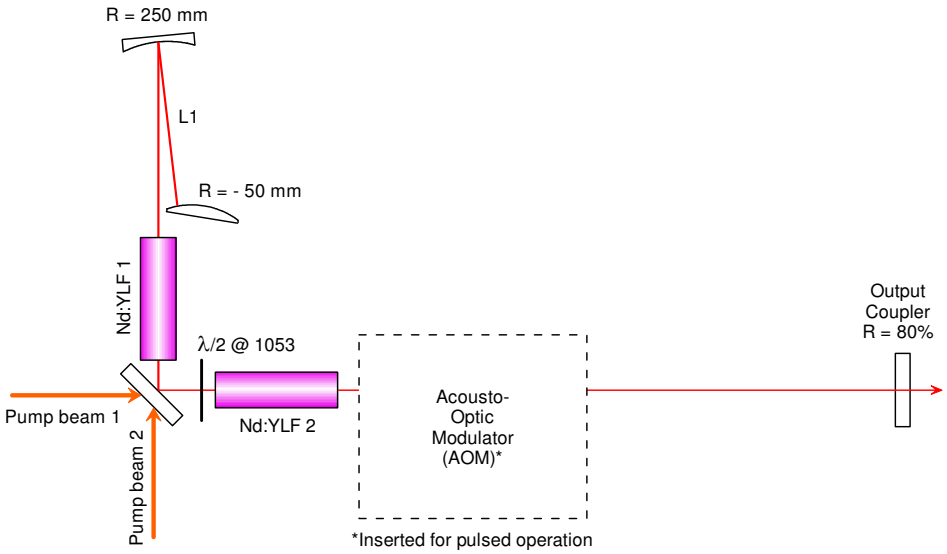

Fig. 5. Resonator setup for the CW and the *Q*-switched experiments.

#125628 - $15.00 USD Received 17 Mar 2010; revised 14 May 2010; accepted 16 May 2010; published 15 Jun 2010

The folding mirror M_2 was mounted on a translation stage, so that the short-arm length L_1 could be fine tuned during operation. In this way, it was possible to adjust the resonator during operation at full pump power for optimum beam quality and efficiency.

An additional advantage of this resonator is the fact that it becomes unstable for stronger negative thermal lensing. This induces high losses for the π-polarization, which has a stronger negative thermal lens than the σ-polarization [10,18], and naturally forces the laser to operate on the σ-polarization at 1053 nm.

While the σ-polarization has a very weak thermal lens, it is strongly astigmatic [2]. In order to compensate for this astigmatism, the same scheme as discussed in [2] was used. Nd:YLF crystal 1 was orientated with its c-axis vertical and crystal 2 with its c-axis horizontal, with a λ/2 plate positioned between the crystals. In this way, the astigmatism of the thermal lenses is compensated, while the polarization with respect to the c-axis is the same in both crystals.

5. Experimental results

5.1 CW results

The CW laser was optimized at full pump power, but not re-adjusted at lower powers. It had a pump power threshold of 9.5 W emitted from the pump delivery fiber and a maximum output power of 60.3 W at 158 W of diode pump power (Fig. 6). A linear regression using all output power values above 10 W yields a slope efficiency of 44% with respect to diode power (49% and 52% with respect to incident and to absorbed pump power, respectively). The regression intersects the x-axis at 20 W of incident pump power. Theoretical values for slope and threshold were calculated using the analytical equations from [26]. The results fit very well when assuming resonator losses of 2% and $\eta_p = 0.75$ (dashed line in Fig. 6). The M^2-values could not be measured at the time of the experiments, due to a fault in the M^2 measurement system. However, the measured output beam profile appeared almost perfectly Gaussian, even at full power (Fig. 7), indicating fundamental-mode operation. The laser was stable during operation and the output power was only limited by the available pump power. It operated on the σ-polarization at all powers.

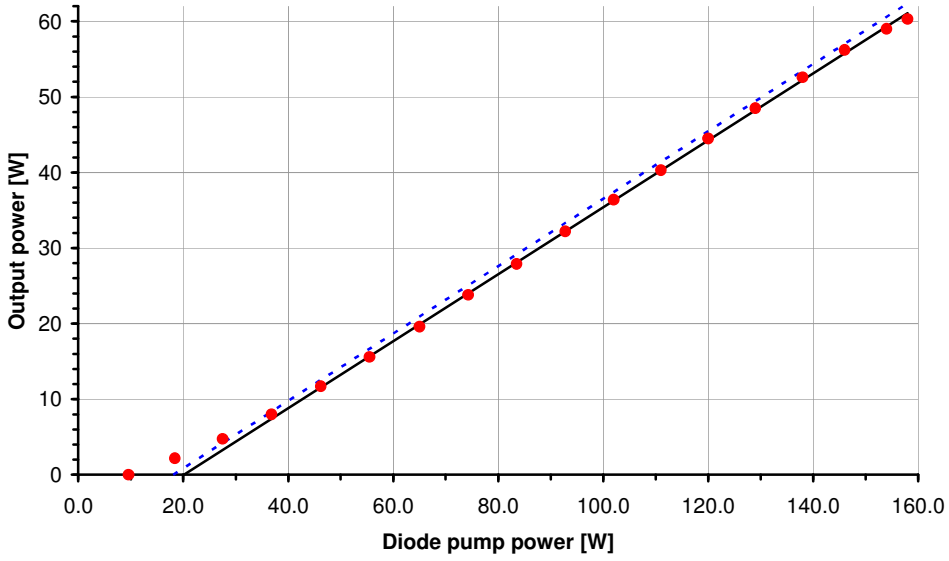

Fig. 6. Output power of the CW laser versus pump power from the laser diode. The red dots are measured experimental values, the solid black line is a linear regression for output powers above 10 W and the dashed line shows the theoretical values for $\eta_p = 0.75$ according to [26].

#125628 - $15.00 USD Received 17 Mar 2010; revised 14 May 2010; accepted 16 May 2010; published 15 Jun 2010

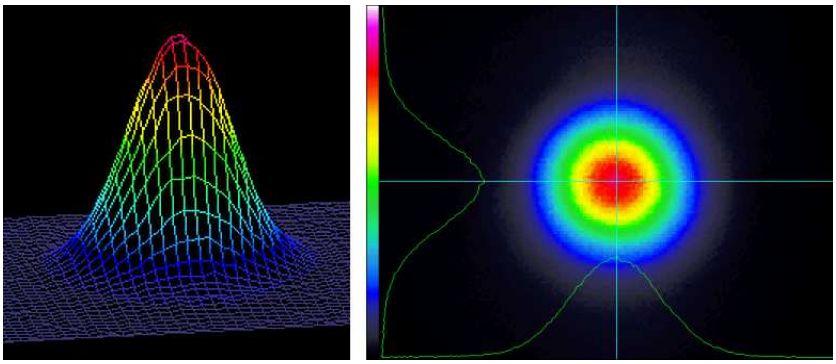

Fig. 7. Beam profile of the CW laser at full power (60.3 W output), detected with a 1/2" LaserCam IIID beam diagnostics camera from Coherent (6.4 x 4.8 mm^2 CCD sensor with 736 x 484 pixels resolution).

5.2 Pulsed operation

The relatively long resonator length increases the pulse length to avoid optical damage at low repetition rates. In addition, it leads to a longer pulse build-up time, which ensures that the Acousto-Optic *Q*-switch has sufficient time to switch fully open before the pulse builds up to a significant power level.

Since the laser resonator is unstable for a strong negative thermal lens, operation on the π-polarization is naturally suppressed and the AOM only needs sufficient loss to suppress operation on the σ-polarization. For these experiments, a Gooch & Housego fused-silica AOM with 3 mm active aperture and integrated driver was used (model QSD27-3C-K-L3). The AOM diffraction loss was measured outside the cavity to be ~65%. This is more than the theoretically required loss of 54%, and it was concluded that the AOM loss should be sufficient to suppress lasing even at full pump power and low repetition rates. For the pulsed operation experiment, the laser was operated at full pump power with different pulse repetition rates, starting at a high repetition rate and then slowly reducing the repetition rate. An average power of 59.1 W was achieved at 30 kHz, which decreased to 52.0 W at 5 kHz, corresponding to 10.4 mJ per pulse. The FWHM pulse lengths ranged from 76 ns at 6 kHz to 285 ns at 30 kHz.

Unfortunately, one of the two Nd:YLF crystals fractured at 5 kHz, so that the experiment could not be continued to even lower repetition rates. The fractured crystal had a crack of about 10 mm depth on the pumped end, indicating thermal fracture. No optical damage was observed. We estimated the maximum stress in the crystal by using Eq. (2).33) of [33]. This is a corrected version of Eq. (1) in [11], which takes the Poisson's ratio into account. With the same thermo-mechanical parameters as in [11], but with a pump absorption coefficient of 1 cm^{-1} and a fractional heat load of 24% due to the quantum defect, the theoretical maximum stress in the crystal is 39 MPa. This is just under the thermal fracture limit of 40 MPa given in [11]. Therefore, a small increase in thermal load due to upconversion at lower repetition rates can lead to fracture. The second crystal remained undamaged despite the fact that oscillation stopped completely when the first crystal fractured. This could be due to variations in the doping concentration, typically caused by a doping gradient in low-doping Nd:YLF boules.

The theoretical average power and pulse energy versus repetition rate were calculated using a formalism similar to that used by Coluccelli et al. [21]:

$$E = P_{cw}\tau\left(1 - e^{-\frac{1}{f\tau}}\right)\xi, \text{with } \xi = \left(\frac{n_\infty - n_f}{n_\infty - n_{th}}\right), \tag{7}$$

where τ is the upper laser level lifetime and *f* is the pulse repetition frequency. ξ is a numerical factor dependent on the population inversion at threshold (n_{th}), the repetition rate dependent

#125628 - $15.00 USD Received 17 Mar 2010; revised 14 May 2010; accepted 16 May 2010; published 15 Jun 2010

inversion after a Q-switched pulse (n_f) and the inversion after an infinitely long pumping time (n_∞). For our laser, with a pump power threshold of 10 W, this factor is 1.07 for repetition rates up to 5 kHz and then slowly decreases to 1.03 at 30 kHz.

Figure 8 shows the measured average power and energy per pulse versus repetition rate, together with the theoretical values according to Eq. (7) and the results of a numerical single-cell plane-wave rate equation model of the laser [33,34]. Measured, simulated and theoretical values agree very well, with virtually no sign of lifetime quenching, even at 5 kHz. This demonstrates that our design process worked well and that we can expect pulse energies close to the theoretical value at lower repetition rates, if the thermal fracture can be overcome.

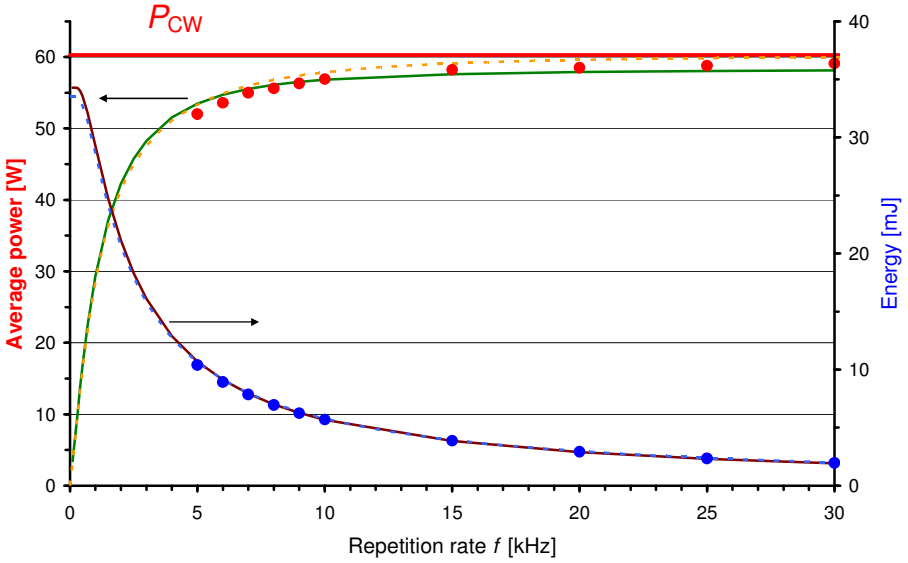

Fig. 8. Average power (red, left y-axis) and pulse energy (blue, right y-axis) vs. pulse repetition rate. The dots are measured experimental values while the dashed line represents calculated theoretical values and the solid line numerical simulation results from a plane-wave rate equation model.

6. Summary and conclusions

A simple formalism to estimate the unsaturated gain of an end-pumped laser medium was developed. This was used to optimize the pump and laser beam size in a continuously end-pumped Q-switched Nd:YLF laser for good performance at low repetition rates. A resonator design incorporating a scheme to compensate for the astigmatic thermal lens was used to achieve a large fundamental laser mode size. With this configuration, up to 60.3 W of CW power was achieved and more than 50 W average power when Q-switched between 5 and 30 kHz.

New experiments with four crystals of even lower doping concentration and utilizing the natural doping gradient in the crystal are currently being performed. Initially, an output power of 87 W was achieved in CW operation with four 75 W pump diodes [35]. We believe that the approach presented here has the strong potential to open up the route to power scaling of end-pumped Nd:YLF lasers to well above 100 W average power and ~50 mJ per pulse while maintaining TEM_{00} beam quality.

#125628 - $15.00 USD Received 17 Mar 2010; revised 14 May 2010; accepted 16 May 2010; published 15 Jun 2010